ORIGINAL ARTICLE

Analysis of vibration reduction mechanism for variable pitch end mills

Wanying Nie[1] · Minli Zheng[1] · Haibin Yu[1] · Shicheng Xu[1] · Yuexiu Liu[1]

Abstract
The development of the machining technology is restricted by the problems of serious vibration and low system stability. The variable pitch cutter has certain vibration reduction property due to the unequal pitch angles. In this work, firstly, according to the features of the structure of the variable pitch end mill, the cutting mechanism is analyzed, and a theoretical model of the dynamic cutting force is developed. Secondly, the cutting force coefficients of the model are determined based on the test of hardened steel for verifying the significance of the theoretical model. Then, the time–frequency characteristics and vibration reduction mechanism of variable pitch end mills are analyzed. The frequency characteristics of different types of pitch angle end mills are also explored by the spectrum analysis. Finally, based on the energy and variance methods of the amplitude, the single-objective optimization of the pitch angle is carried out, where the spectrum lines are found evenly distributed, and the optimal result is 80°-97°-100°-83°. For satisfying the machining requirements, the pitch angle of the variable pitch end mill is reasonably selected to reduce the amplitude of the forced vibration, which can play an important role in reducing the vibration of the tool and improving its cutting stability. The superior vibration reduction tool is of great significance for improving the processing technology and accelerating the development of the manufacturing industry.

1 Introduction

With the increasingly complex structures of products, the requirements of machining accuracy and quality consistency are also being increased continuously, leading to increasing difficulties in machining materials which urgently require high-performance tools. It is difficult to improve the surface quality of a workpiece due to serious vibration. In order to reduce the cutting vibration from the point of tool design, Slavicek [1] first proposed the design of the variable pitch cutter for vibration suppression. Altintas et al. [2] and Sims et al. [3] proposed a model for variable pitch cutting predicting stability in the frequency domain. Budak [4, 5] and Turner et al. [6] studied the time-domain stability of the variable pitch mill and developed a dynamic model for aluminum alloy. Olgac and Sipahi [7] explained the phenomenon that the variable pitch mill can restrain cutting chatter from physical and mathematical perspectives. At the same time, the research on vibration problems in the machining process is conducted in more depth. Zhou et al. [8] presented an approach for systematic singularity analysis of cutting force and vibration in feature extraction. Li et al. [9] developed a chatter model of single-degree of freedom by taking nonlinear hysteretic and exciting force into account. Freyer et al. [10] combined with piezoelectric transducers to actively detect tools and control vibration. Suyama and Diniz [11] analyzed the effect of tool vibration on insert wear during the turning of hardened steel. Lawrance et al. [12] investigated the relationship between tool vibration and material variation of hardened steel during the drilling

✉ Minli Zheng
minli@hrbust.edu.cn

Wanying Nie
670122439@qq.com

Haibin Yu
Quentina_YU@hrbust.edu.cn

Shicheng Xu
1126888040@qq.com

Yuexiu Liu
1944366152@qq.com

1   College of Mechanical and Power Engineering, Harbin University of Science and Technology, Harbin 150080, China

process and determined its effect on cutting performance. Based on the closed-loop frequency response and dynamics model, Wu J et al. [13, 14] studied the vibration problem of the motion command, and planned the critical angle and position compensation. Yu et al. [15] studied the influence of the cutting force coefficient on the spindle speed and axial cutting depth, and optimized the stability lobe diagram of different cutting parameters. Shirase et al. [16] observed that the variable pitch cutter has a better vibration damping performance in comparison with the cutting performance of an ordinary cutter. Tang [17] established the eccentricity equation of unequal tooth cutter is based on the dynamic balance theory and expounded the balance problem of asymmetric structure cutter. Sellmeier et al. [18] presented a model of the cutting force and surface machining error of the variable pitch end mill. Yusoff and Sims [19] and Otto et al. [20] explored the stability of variable pitch cutting and optimized the cutter parameters. Huang [21] and Jin [22] developed another dynamic model of the variable pitch mill by analyzing the cutting stability for titanium alloy. Alex and Zoltan [23] studied the vibration reduction mechanism of unequal tooth cutters in face milling.

The superiority of the damping performance of variable pitch end mills has been widely studied. However, the mechanism reducing the tool vibration still lacks certain analysis in hardened steel materials. In this paper, the cutting force model of the variable pitch end mill is studied by taking into account the problem of multi-time delay caused by the change in the pitch angle. The cutting force coefficients are analyzed, and the experimental and simulation results are compared, and the relationship between the spectrum characteristics of the mill and the mechanism of the forced vibration reduction is established. According to the amplitude diagram of the cutter in the frequency domain, the pitch angle is optimized by taking the minimum energy and variance as the objective, so that the damping performance of the mill can be continuously improved under certain conditions.

2 Dynamic model of cutting force based on semi-analytical method

As an effective strategy to suppress vibration [24], the variable pitch end mill causes a difference in the cutting time delay due to the unequal angle distribution between teeth. It changes the dynamic cutting force and contact angle during cutting. Accordingly, different teeth bear different chip loads. Figure 1 displays the axial expansion diagram of the variable pitch end mill with the contact area diagram of the tool-workpiece Fig. 1a, where N ($N = 4$) is the number of teeth in the end mill, D is the diameter, β is the helix angle,

Fig. 1 Schematic diagram of the variable pitch end mill with two degrees of freedom (**a**) contact area diagram of the tool-workpiece, (**b**) schematic diagram of the cutting process (**c**) force model
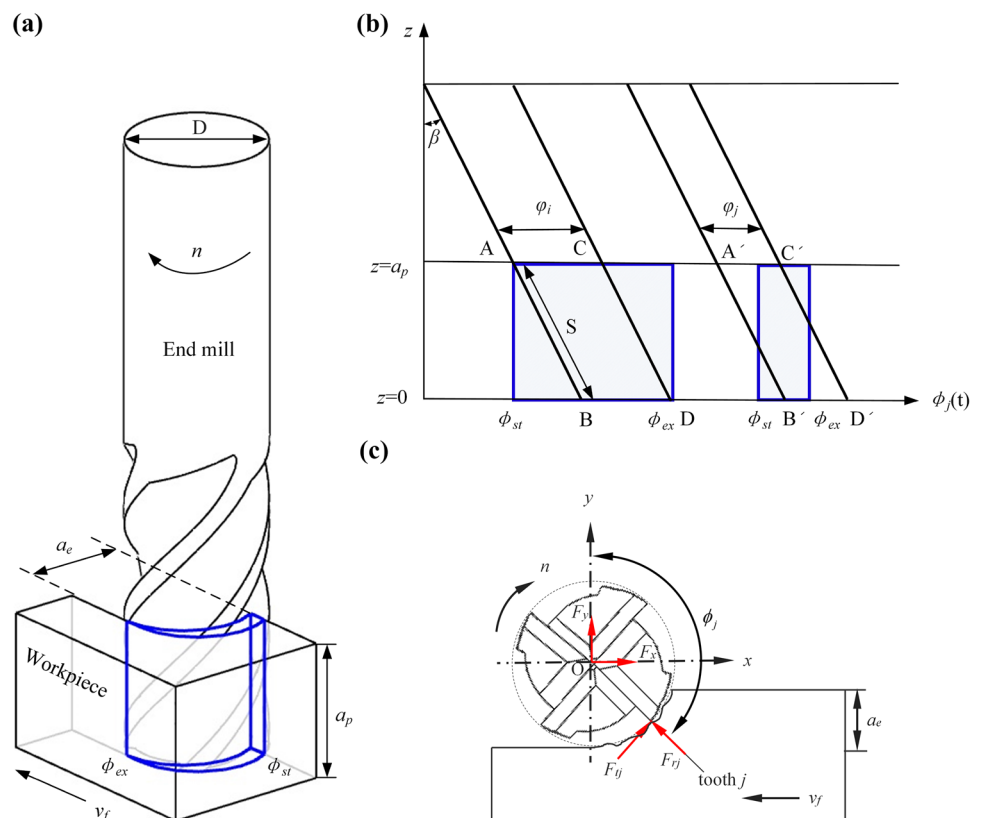
and φ_j ($j = 1, 2, 3, 4$) is the pitch angles. The blue part is the amount of material removed, a_p is the depth of milling, a_e is the width of milling, v_f is the feed of milling, n is the milling speed, and S is the contact length of the cutting edge, where $S = \frac{z}{\cos\beta}$. In the actual cutting process of the variable pitch end mill, the relationship of the pitch angles determines the specific situation of multi-tooth involved in the cutting. When $a_e > R(1 - \cos\varphi)$, the helical edge of end mill engages multiple teeth in the cutting. Figure 1b shows the schematic diagram of the cutting process, where the blue solid line represents the processing area of the workpiece, and the black thick solid line represents the cutting edge with ϕ_{st} as the cut-in angle and ϕ_{ex} as the cut-out angle. As show the figure, the cutter teeth in the multi-tooth cutting are divided into two categories: complete cutting teeth and partial cutting teeth, which mainly depend on the axial cutting depth a_p, helix angle β, radius r, cut-in angle ϕ_{st} and cut-out angle ϕ_{ex}. When $a_p > (\phi_{ex} - \phi_{st})R\arctan\beta$ in Fig. 1b, the situation marked by ABCD occurs, otherwise that marked by A′B′C′D′ occurs. There are three different situations in the cutting process: partial cutting-in, complete cutting-in and partial cutting-out.

According to the force model of the variable pitch end mill (as shown in Fig. 1c), ϕ_j is the contact angle of tooth j. The micro-element force acting on cutter tooth j is expressed as follows:

$$\begin{aligned} dF_{tj} &= K_{tc}h(\phi_j(z))dz + K_{te}ds \\ dF_{rj} &= K_{rc}h(\phi_j(z))dz + K_{re}ds \\ dF_{aj} &= K_{ac}h(\phi_j(z))dz + K_{ae}ds \end{aligned} \tag{1}$$

where K_{tc}, K_{rc} and K_{ac} are, respectively, the tangential, radial and axial coefficients of the cutting force. K_{te}, K_{re} and K_{ae} are, respectively, the tangential, radial and axial coefficients of the edge force. dF_{tj}, dF_{rj} and dF_{aj} are, respectively, the tangential, radial and axial cutting forces of the micro-element cutting edge of cutter tooth j. $\phi_j(z)$ is the contact angle of cutter tooth j at the axial cutting depth z, and $h(\phi_j(z))$ is the dynamic cutting thickness.

$$\phi_j(z) = \begin{cases} wt - k_{\beta z} = \frac{n\pi t}{30} - k_{\beta z} & j = 1 \\ wt - \sum_{j=2}^{N} \varphi_j - k_{\beta z} & j = 2, \ldots \ldots N \end{cases} \tag{2}$$

The lag angle of cutter tooth j, relative to the tip of the cutter at the cutting depth z, can be expressed as $\theta = \frac{2z\tan\beta}{D} = k_{\beta z}$.

$$h(\phi_j(z)) = f_{zj}\sin(\phi_j(z)) + \Delta x_j\sin\phi_j(t) + \Delta y_j\cos\phi_j(t) \tag{3}$$

where $f_{zj} = f_r\frac{\varphi_j}{2\pi}$ is the feed per tooth of end mill tooth j with f_r as the feed per revolution of end mill. Δx_j and Δy_j are, respectively, the displacement of the current cutter tooth due to the vibration, $\begin{Bmatrix} \Delta x_j(t) \\ \Delta y_j(t) \end{Bmatrix} = \begin{Bmatrix} x(t) - x(t - \tau_j) \\ y(t) - y(t - \tau_j) \end{Bmatrix}, \tau_j = \frac{30\varphi_j}{\pi n}$ is the time delay of the current cutter tooth j.

According to the single-tooth cutting force model, the instantaneous cutting force model of the variable pitch end mill with multiple teeth participating in the cutting process is obtained as follows:

$$[F_t\ F_r\ F_a]^T = g(\phi)\left[\sum_{j=1}^{N}F_{tj}\ \sum_{j=1}^{N}F_{rj}\ \sum_{j=1}^{N}F_{aj}\right]^T \tag{4}$$

where $g(\phi_j(z))$ is the step response function, which indicates whether the cutter teeth participate in the cutting.

$$g(\phi_j(z)) = \begin{cases} 1 & \varphi_{st} \le \phi \le \varphi_{ex} \\ 0 & else \end{cases} \tag{5}$$

When the contact angle of the cutter tooth lies between the cut-in angle and cut-out angle, the cutting edge takes part in the cutting. The cut-in angle and cut-out angle during the down milling can be expressed as follows:

$$\begin{aligned} \phi_{st} &= \pi - \cos^{-1}\left(1 - \frac{a_e}{R}\right) \\ \phi_{st} &= \pi \end{aligned} \tag{6}$$

In the actual processing situation, the cutting force of the end mill is monitored by a dynamometer, which mainly measures the forces in the x, y and z directions of the machine tool. Through coordinate transformation, the cutting forces of the variable pitch end mill in feed, normal and axial direction are transformed into the x–y–z coordinate system as follows:

$$F = \begin{Bmatrix} F_x \\ F_y \\ F_z \end{Bmatrix} = g(\phi)\begin{bmatrix} -\cos\phi & -\sin\phi & 0 \\ \sin\phi & -\cos\phi & 0 \\ 0 & 0 & 1 \end{bmatrix}\begin{Bmatrix} F_t \\ F_r \\ F_a \end{Bmatrix} \tag{7}$$

The radial and axial cutting forces of single tooth can be expressed as:

$$\begin{aligned} F_{rj} &= K_r F_{tj} \\ F_{aj} &= K_a F_{tj} \end{aligned} \tag{8}$$

where K_r and K_a are, respectively, the proportional coefficients of the radial and axial cutting forces for different materials, which can be expressed as $K_r = \frac{K_{rc}}{K_{tc}}$ and $K_a = \frac{K_{ac}}{K_{tc}}$.

The dynamic cutting force is developed due to the dynamic cutting thickness. Accordingly, the tangential cutting force of a single tooth of the variable pitch end mill can be expressed as:

amplifier, data acquisition system, acceleration sensor and data processing software.

In this paper, ten groups of single factor tests were carried out for minimizing the influence of controllable factors on

$$
\begin{aligned}
F_{tj} &= \int_{z_1}^{z_2} \left(K_{tc} \left(f_r \frac{\varphi_j}{2\pi} \sin \phi_j(z) + \Delta x_j \sin \phi_j(z) + \Delta y_j \cos \phi_j(z) \right) + \frac{K_{te}}{\cos \beta} \right) dz \\
&= -\frac{D}{2 \tan \beta} \int_{\phi_j(z_1)}^{\phi_j(z_2)} \left(K_{tc} \left(f_r \frac{\varphi_j}{2\pi} \sin \phi_j(z) + \Delta x_j \sin \phi_j(z) + \Delta y_j \cos \phi_j(z) \right) + \frac{K_{te}}{\cos \beta} \right) d\phi_j
\end{aligned}
\tag{9}
$$

Based on the analysis of the cutter tooth time delay and force in the machining process of the milling cutter, the instantaneous cutting force model of the variable pitch end mill is developed, the cutting mechanism of the mill is determined, and the relationship between the pitch angle and cutting force is established.

3 Testing of CrMoV hardened steel

The instantaneous cutting force is determined by applying an analytical method to a discrete model of the cutting tool. The accuracy of the predicted cutting force depends largely on its coefficients. A hardened steel has the characteristics of high strength, high hardness, and so on. It is a typically difficult material for machining, and vibration is prominent in its milling process. In order to verify the reliability and improve the theoretical accuracy of the model, the coefficients of cutting force are estimated by using the measured cutting force.

The testing site diagram is shown in Fig. 2, the test tool is carbide, and its geometry is listed in Table 1. The composition and properties of the material are listed in Tables 2 and 3, respectively. The equipment includes VDL-1000E CNC machining center, Kistler rotary dynamometer, charge

the results of the test. The testing plan is shown in Table 4. Since the material properties of the workpiece are not uniform, the measurement of the cutting force is repeated for 10 times for each group of cutting parameters. The cutting forces of the third, fifth and seventh time are monitored, and their average is taken as the final cutting force of the group parameter.

Based on the theoretical model of the cutting force of the variable pitch end mill, the cutting force coefficients of the model are first measured by a rapid calibration method, then those are related to many factors such as cutting parameters, tool-workpiece material matching, tool geometry and machining system, and the influence of every factor is complex. In 1–5 groups and 6–10 groups of the testing plane, the other three cutting parameters are kept fixed, the feed rate and the cutting depth are increased linearly, respectively. The instantaneous cutting forces F_x, F_y and F_z are measured by the dynamometer. Due to the high axial stiffness of the system, the cutting forces in the x and y directions are discussed, and the regression analysis is conducted (as shown in Fig. 3), where the fitting degrees of the test data are found to be 98.6%, 98.6%, 98.7% and 99.7%, respectively. The cutting force coefficients are time-varying, the fitting results are averaged. Finally, the cutting force coefficients $K_{tc} = 7360$ N/mm² and $K_{rc} = 3110$ N/mm²,

Fig. 2 Testing site diagram (**a**) end section of the variable pitch end mill (**b**) hardened steel material (**c**) equipment (**d**) testing system
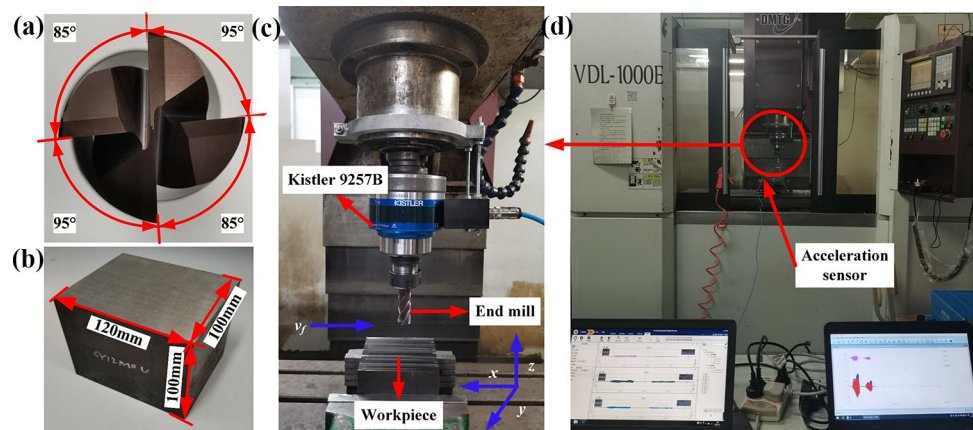
Table 1 Carbide end mill geometry

Diameter (mm)	Number of flutes	Edge length (mm)	Total length (mm)	Rake angle (°)	Pitch angle (°)	Helix angle (°)	Nose radius (mm)
20	4	38	104	15	85–95–85–95	40	0.8

Table 2 Chemical composition of hardened steel (CrMoV)

Component	C	Si	Mn	P	S	Cr	V	Mo	Ni	Cu
Content (%)	1.55	<0.40	<0.40	<0.03	<0.03	10.50	0.25	0.40	<0.25	<0.30

Table 3 Physical properties of hardened steel (CrMoV)

Hardness (HRC)	Elastic modulus E (GPa)	Density ρ (g/cm^3)	Specific heat capacity C (J/Kg.K)	Conductivity k (W/m.K)	Poisson's ratio u
60	223	7.70	0.46	20	0.27

Table 4 Testing plan and results

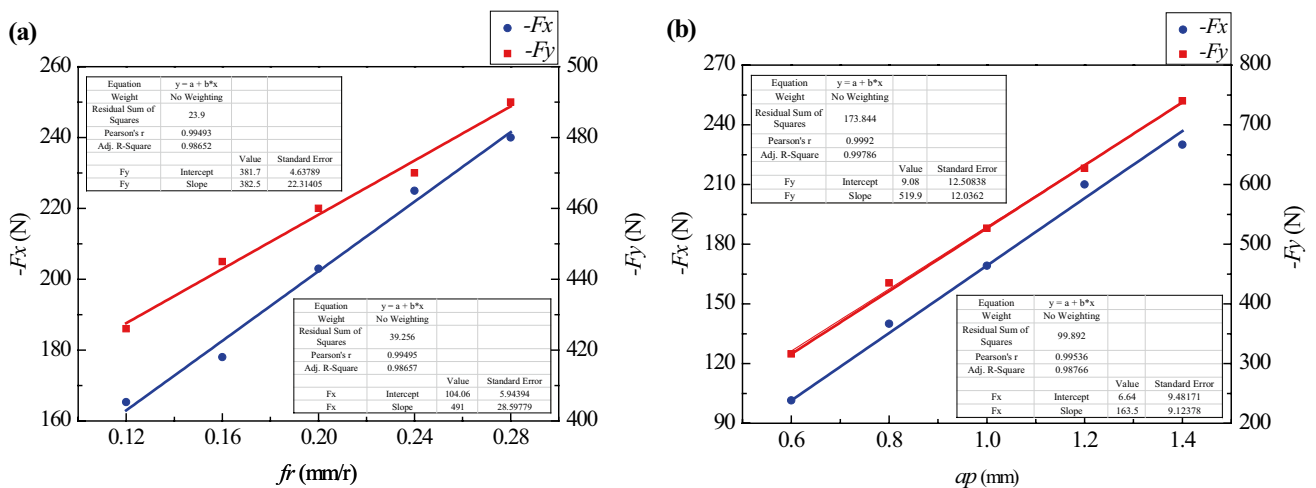| Group number	Rotating speed n (r/min)	Cutting depth a_p (mm)	Cutting width a_e (mm)	Feed rate f_r (mm/r)	Cutting force $-F_x$ (N)	Cutting force $-F_y$ (N)
1	2000	1	0.5	0.12	165.3	426.0
2				0.16	178.5	445.6
3				0.20	203.6	460.1
4				0.24	225.8	470.5
5				0.28	240.0	490.0
6	2500	0.6	1	0.20	101.5	316.1
7		0.8			140.4	425.5
8		1.0			169.2	526.8
9		1.2			210.0	627.2
10		1.4			230.9	740.6

Fig. 3 Relationship between cutting force and cutting parameters (**a**) feed rate in the x and y direction and (**b**) cutting depth in the x and y direction

and the cutting edge force coefficients $K_{te} = 170$ N/mm^2, and $K_{re} = 254$ N/mm^2 are obtained.

Figure 4 shows the vibration acceleration diagrams of the fifth and tenth groups in the milling test. It can be seen from the figure that the milling process of hardened steel is still relatively stable under the condition of the maximum cutting parameters, which meets the basic conditions for the theoretical model of the milling force. The obtained cutting force coefficients of the hardened steel (CrMoV) are used in the theoretical model of the cutting force of the variable pitch end mill, and the significance of the model is verified. Figure 5 shows the testing result diagram. Due to the unequal pitch angles, there is a difference between the peak values of the dynamic cutting force at two adjacent teeth. It can be seen that the dynamic trend of the cutting force is in good agreement in the figure. The experimental average results are $F_x = -203.6$ N and $F_y = -460.1$ N, and the simulation values are $F_x = -186.7$ N and $F_y = -443.5$ N, having differences of 8.3% and 3.6%, respectively. It indirectly indicates that the theoretical model of the cutting force of the variable pitch end mill has certain prediction accuracy. From the FFT diagram, it can be seen that the fundamental frequency for the frequency domain amplitude distribution is the same in the x and y directions under the forced vibration controlled by the milling force.

4 Simulation results and discussion

The cutting force model of the variable pitch end mill is formed with the pitch angles, cutting force coefficients for materials and cutting parameters. Based on the above testing conditions, the influence of different types of changes in the pitch angle on the time-domain characteristics of the cutting force and the corresponding spectrum are analyzed. The amplitude spectrum describes the outline and shape of the exciting force signal, and the phase spectrum describes the position of the signal. The harmonic component of amplitude spectrum determines the degree of vibration, which indirectly reveals the relationship between the pitch angle of the end mill and cutting vibration, and provides the theoretical basis for the damping of the cutter.

According to the cutting mechanism of the variable pitch end mill, the feed rate of each tooth is different at different distributions of the pitch angle. The cutting force of each tooth is different, which constantly changes the peak of the force. According to Eq. (10), there is a linear positive correlation between the cutting force and the pitch angle, leading to different loads on cutting edges and premature wear failure on the cutting edge with larger pitch angle. Therefore, the influence of the difference in the pitch angle on the machining performance of the cutter teeth should be considered in the analysis of the pitch angle. When the difference angle between teeth $j + 1$ and j is $\Delta \varphi$, the relationship between the static load difference of the two teeth is expressed as follows:

$$\Delta F = K_c a_p \frac{\Delta \varphi}{2\pi} f_r \sin\phi \tag{10}$$

Based on the basic theory of Fourier series generation, the cutting force model is analyzed in the frequency domain, and the machining condition is determined as down-milling. The cutting parameters are D = 20 mm, n = 2000r/min, $f_r = 0.12$ mm/r, $a_p = 1$ mm, $a_e = 10$ mm, and the material cutting force coefficients are the same as above. There are four different types of parameters for pitch angle distribution in the variable pitch end mill, which are equal pitch angle 90°-90°-90°-90°, symmetrical pitch angle 85°-95°-85°-95° and linear pitch angle 75°-85°-95°-105°. The influence of the pitch angle of the milling cutter on the corresponding spectrum is confirmed. It is shown in Fig. 6 by comparing the characteristics of three different types of inter-tooth angles in the frequency domain of the cutting force.
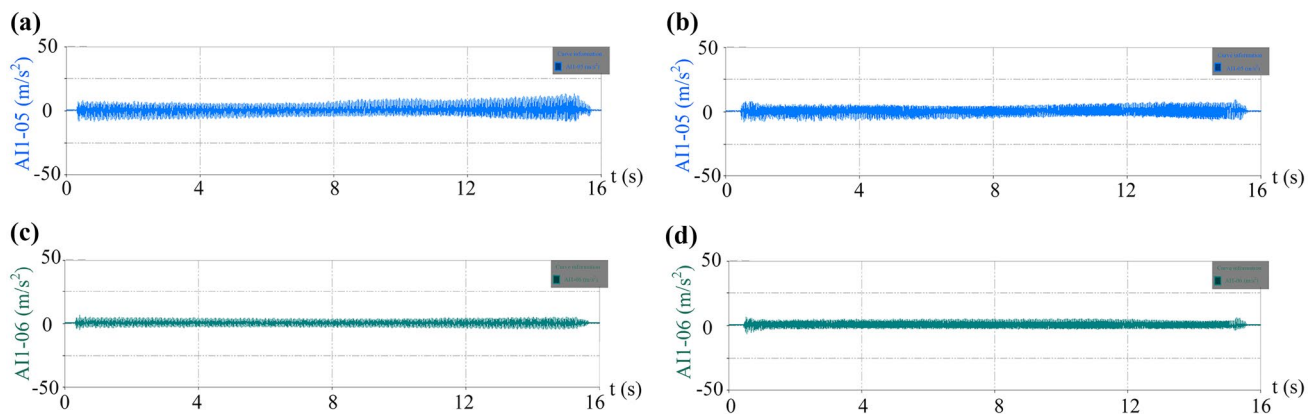

Fig. 4 Acceleration diagram of the milling vibration (**a**) and (**c**) show the five group in the x and y direction, (**b**) and (**d**) show the ten group in the x and y direction

Fig. 5 Testing result diagram, comparison diagram of milling force test and model simulation (**a**) shown in the *x* direction, (**b**) shown in the *y* direction, and FFT diagram of cutting forces (**c**) in the *x* and *y* direction
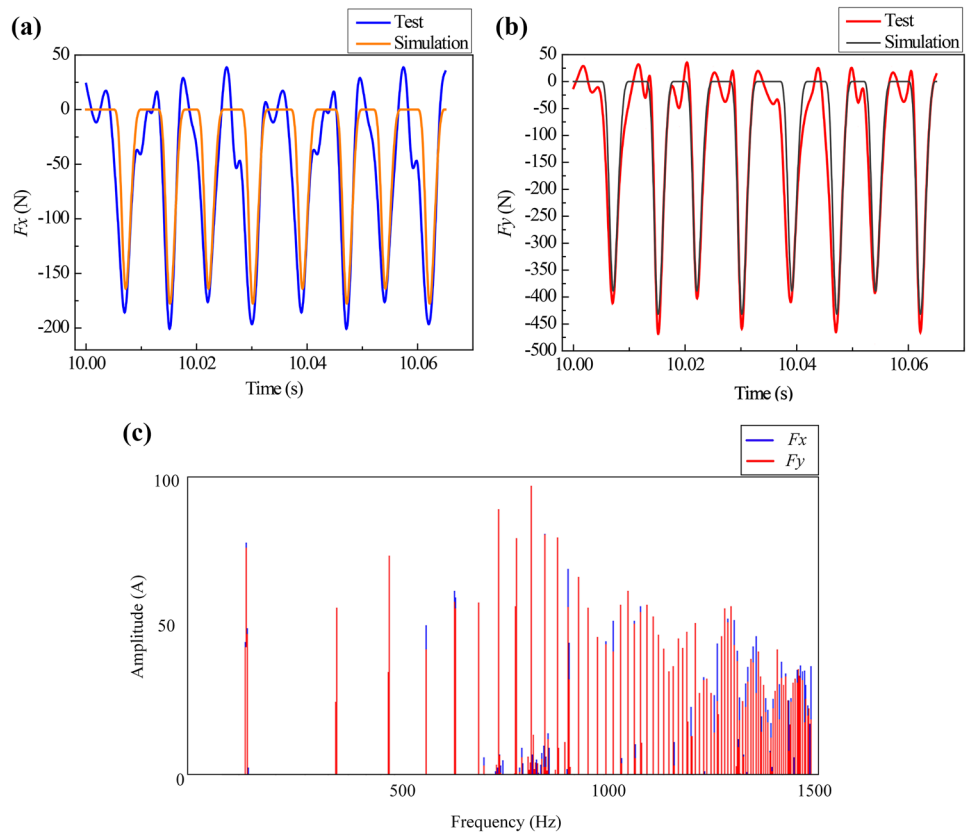

Figure 6 shows that the characteristics of end mills are different for different inter-tooth angles of the cutting force in the frequency domain. Due to different trends of the pitch angle and different cutting parameters of each tooth, the extreme cutting force and the time delay interval are different. At the same time, when the period of the milling cutter changes from low to high, the amplitude spectrum is distributed in a wider range of frequencies, and the harmonic component is reduced. For example, the extreme values of the cutting force spectrum of the end mills with different tooth angles are reduced compared to those with equal-tooth end mills, respectively, by 2.1%, 26.2% and 2.6%, 5.6% in the *x* and *y* direction. Therefore, when the pitch angle of the variable pitch end mill tends to be asymmetrical, the cutting force spectrum of the milling cutter becomes more dispersed and uniform, resulting in smaller tool forced vibration and higher cutting stability under the same cutting conditions.

5 Optimization of end mills

Moreover, the structural rigidity of thin-walled parts is weak, which is easy to be affected by vibration. Therefore, the pitch angle of the variable pitch end mill is optimized by taking the milling vibration as the index for evaluating

the tool and the vibration minimization of the process system as the objective function. When the frequency response function $S_S(f)$ and exciting force $A_e(f)$ of the machine tool-workpiece system are known, the relative vibration amplitude spectrum $S_R(f)$ between the tool and the workpiece can be expressed as follows:

$$S_R(f) = A_e(f) \times S_S(f) \tag{11}$$

In the actual milling process, when the cutting tool is suitable for different processing conditions, the response function of the system frequency under different conditions cannot be obtained in real time. In order to make the cutting tool meet all the processing conditions, the response function of the system frequency becomes a horizontal line (default) based on the statistical angle $S_S(f) = const$. The cutting force spectrum of the variable pitch end mill needs flatness to minimize its vibration.

The pitch angle of the end mill is taken as the design variable, and the sum of the harmonic energy (energy method Eq. 12) and the square of the amplitude deviation (variance method Eq. 13) of the cutting force are taken as the objective function. The energy method shows the sum of the vibration amplitudes, and the variance method shows the flatness of the vibration amplitude. The optimal distribution of the angle between the teeth is carried out, so that the amplitude
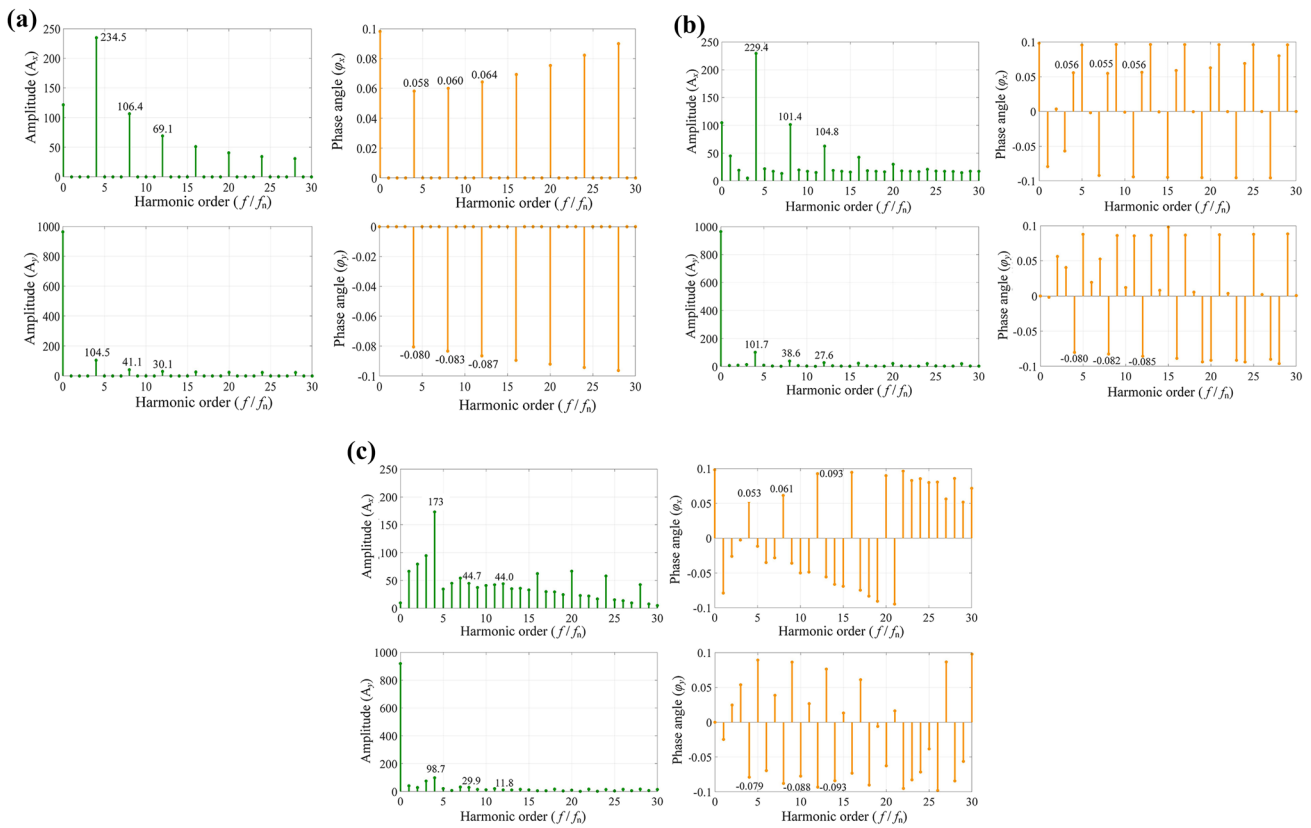
Fig. 6 Spectrum of end mills with different pitch angle for the cutting force simulation (**a**) equal (90°-90°-90°-90°) (**b**) alternating (85°-95°-85°-95°) (**c**) linear (75°-85°-95°-105°)

of the forced vibration is reduced and made flat. Let the vibration reduction performance of the variable pitch end mill reaches the theoretical best state. The objective function is obtained from the energy method and the variance method as follows [25]:

$$E(f) = \sum_{f=1}^{n} A_e(f)^2 = \left(a_1 \sum_{f=1}^{n} F_x(f)^2 + a_2 \sum_{f=1}^{n} F_y(f)^2 \right) \quad (12)$$

$$S^2(f) = \left(\sum_{f=1}^{n} \left(A_e(f) - \frac{\sum_{f=1}^{n} A_e(f)}{n} \right)^2 \right) = \left(a_1 \sum_{f=1}^{n} \left(F_x(f) - \frac{\sum_{f=1}^{n} F_x(f)}{n} \right)^2 + a_2 \sum_{f=1}^{n} \left(F_y(f) - \frac{\sum_{f=1}^{n} F_y(f)}{n} \right)^2 \right) \quad (13)$$

where f is the cutting frequency of the cutter teeth, $A_e(f)$ is the vibration amplitude. a_1 and a_2 $(a_1 + a_2 = 1)$ are

determined by the dynamic stiffness of the machine tool as the weighting coefficients in the x and y directions, respectively. $F_x(f)$ and $F_y(f)$ are the amplitude components of the milling force spectrum in the x and y directions, respectively. n is the harmonic order.

The optimization of the pitch angle is a multi-variable and multi-constrained parameter optimization problem. In order to ensure the convergence of the optimum results, a global search algorithm is adopted to analyze the problem comprehensively, by combining with multiple sets of initial variable values and constraints (Eq. 14).

Table 5 Optimization results of pitch angles

Initial value φ_0 (°)	Upper and lower bounds / Pitch angle difference (°)			Energy method		Variance method	
	φ_{min}	φ_{max}	$\triangle\varphi$	Optimize the pitch angle (°)	Objective function value	Optimize the pitch angle (°)	Objective function value
85-95-85-95	60	120	60	60–118–120–62	2.2359e + 05	60–118–120–62	1.4300e + 05
	60	110	50	60–109–110–81	3.0601e + 05	60–109–110–81	2.0108e + 05
	70	120	50	70–99–120–71	3.4187e + 05	70–96–120–74	2.5670e + 05
	70	110	40	70–109–110–71	3.4389e + 05	70–109–110–71	2.4553e + 05
	60	100	40	62–98–100–100	4.1645e + 05	62–98–100–100	3.0869e + 05
	70	100	30	70–97–100–93	4.6477e + 05	70–97–100–93	3.5551e + 05
	80	110	30	80–90–110–80	4.9936e + 05	80–87–110–83	3.9609e + 05
	80	100	20	80–97–100–83	5.1541e + 05	80–97–100–83	4.1542e + 05
	85	95	10	85–91–95–89	5.9223e + 05	85–91–95–89	5.1335e + 05

$$\sum_{i=1}^{4} \varphi_i = 2\pi \tag{14}$$

$$\varphi_{min} \leq \varphi_i \leq \varphi_{max}$$

where φ_i is the pitch angle of the i-th cutting edge, φ_{min} and φ_{max} are the upper and lower bounds of the inter-teeth angle, respectively.

The global search method depicts that the optimum result has nothing to do with the initial value. The pitch angle of the tool in the cutting force test is taken as the initial value in the optimization process. Different groups of constraints are set. The optimization results are shown in Table 5, where it can be seen that the objective value decreases with increasing pitch difference angle (as shown in Fig. 7). The optimization results are mostly consistent for different objectives. It indicates that the determination of the pitch angle becomes two single-objective optimization problem, which has the characteristics of minimum spectrum energy and flat amplitude. According to Eq. (10), when the difference angle between the teeth falls in a certain range, the load difference of the cutting edge becomes larger. The uneven force on each tooth of the cutter is serious, which may lead to premature failure and deformation of the cutter. Considering the strength requirements of the cutter teeth and the balance of the milling cutter structure, the optimum values under the constraint of 20° pitch angle difference are found as 80°-97°-100°-83°. Figure 8 shows the stability lobe and

the frequency spectrum of the corresponding cutting force, in which limit cutting depth is increased and the amplitude is greatly reduced and the change trend is relatively gentle. The extreme values of F_x and F_y amplitude diagrams are reduced by 30.4% and 8.9%, respectively, compared with equal pitch cutter. Therefore, it can be concluded that the optimum pitch angle can reduce the vibration of the milling cutter and effectively improve the cutting stability.
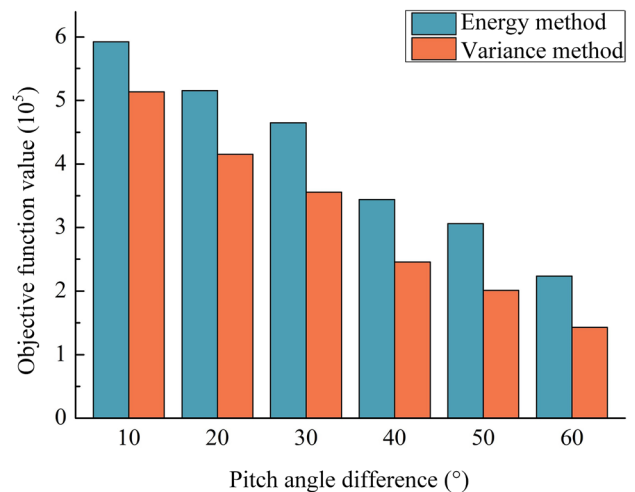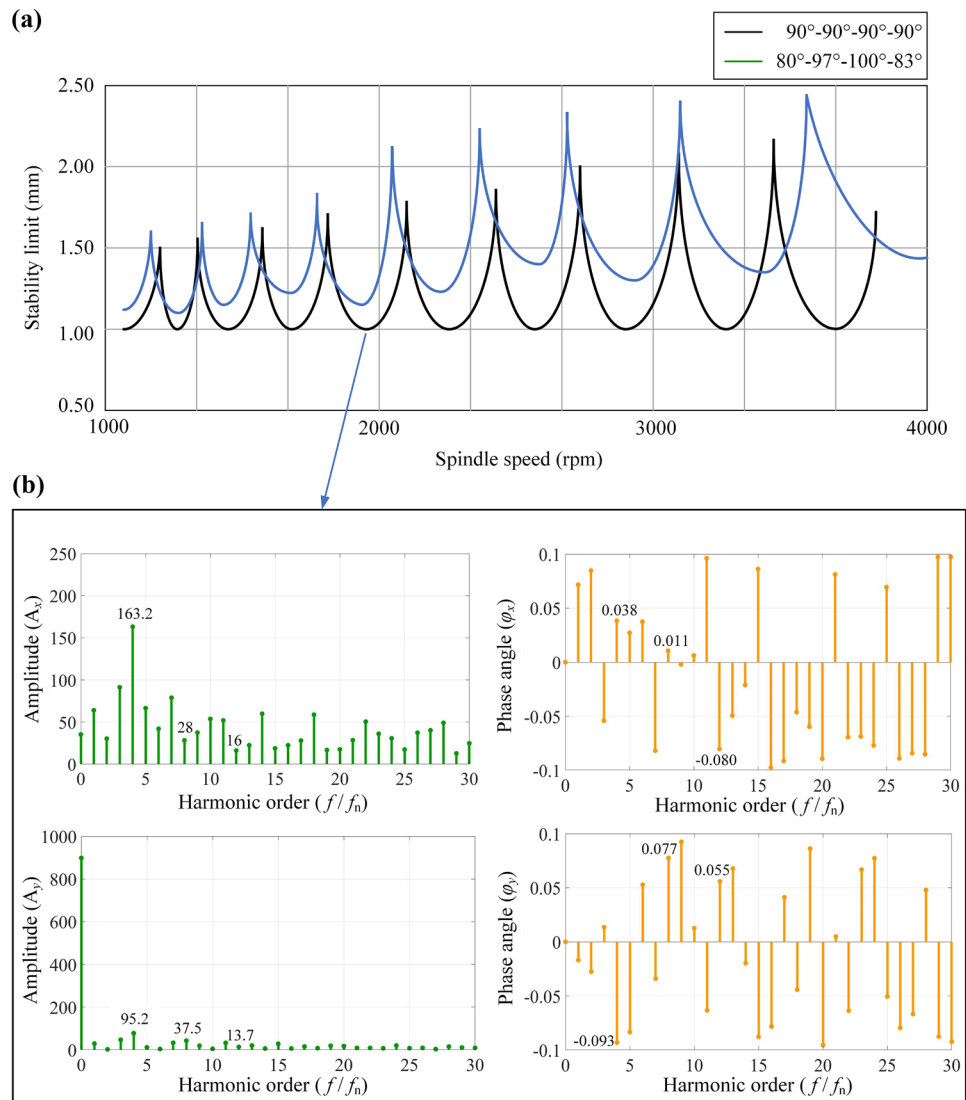

Fig. 7 Relationship between pitch angle difference and objective function value

Fig. 8 Stability picture of end mill with optimal pitch angle (80°-97°-100°-83°) (**a**) lobe diagram (**b**) frequency spectrum

6 Conclusions

In this paper, the variable pitch end mill is investigated. The time delay characteristics and cutting mechanism of the end mill are analyzed, and a cutting force model of the variable pitch end mill is developed. Based on the test with milling hardened steel (CrMoV), the cutting force coefficients are calculated by using the instantaneous cutting force calibration method, and the significance of the cutting force model is verified. This paper studies the time–frequency characteristics of the cutting force of the end mill, and discusses the frequency spectrum of the cutting force under different types of pitch angles. It is found that the pitch angle is the key factor, which leads to the change of the frequency spectrum characteristics of the milling force. The results show that the end mill with asymmetric structure can reduce the maximum amplitude by more than 20% compared with that with a symmetric structure, which has the function of

dispersing harmonic components, indicating that it has better damping performance. At the same time, the pitch angle of the variable pitch end mill is optimized for different objective functions, and the relationship between the optimal distribution of the pitch angle and the objective function is comprehensively analyzed under different constraints. It is found that increasing pitch difference angle leads to the continuous decrease in the objective function. When the pitch difference angle is 20°, the optimization result of the pitch angle is 80°-97°-100°-83°. The extreme values of F_x and F_y spectrum amplitudes are reduced by about 30.4% and 8.9% compared with equal pitch cutter, respectively, which shows that the milling cutter structure has better damping performance. In actual machining, the pitch difference angle should be combined with the cutter design criteria, so as to make the cutter meet certain strength requirements. To sum up, there is a direct relationship between the tooth angle of the variable pitch end mill and the vibration characteristics

of the tool. The optimal structure of the tooth angle of the variable pitch end mill has better cutting stability, which is of great significance to prolong the tool life and improve the machining efficiency. It continuously improves the manufacturing process of key parts and accelerates the flourishing development of key industries.

Declarations

Conflicts of interest The authors declare no conflict of interest.

References

1. Slavicek J (1965) The effect of irregular tooth pitch on stability of milling. Proc Sixth MTDR Conf 15–22
2. Altintas Y, Engin S, Budak E (1999) Analytical stability prediction and design of variable pitch cutters. J Manuf Sci Eng 121(2):173–178
3. Sims ND, Mann B, Huyanan S (2008) Analytical prediction of chatter stability for variable pitch and variable helix milling tools. J Sound Vib 317:664–686
4. Budak E (2003) An analytical design method for milling cutters with non-constant pitch to increase stability, Part 1: Theory. J Manuf Sci Eng 125(1):29–34
5. Budak E (2003) An analytical design method for milling cutters with non-constant pitch to increase stability, Part 2: Application. J Manuf Sci Eng 125(1):35–38
6. Turner S, Merdol D, Altintas Y, Ridgway K (2007) Modelling of the stability of variable helix end mills. Int J Mach Tools Manuf 47:1410–1416
7. Olgac N, Sipahi R (2007) Dynamics and stability of variable-pitch milling. J Vib Control 13(7):1031–1043
8. Zhou C, Guo K, Yang B, Wang H, Lu L (2019) Singularity analysis of cutting force and vibration for tool condition monitoring in milling. IEEE Access 7:134113–134124
9. Li QL, Wang B, Zhao B, Wen BC (2013) Study on stability of machine tool chatter system considering nonlinear hysteretic force. J Mech Eng 49(11):43–49
10. Freyer BH, Theron NJ, Heyns PS, Pickelmann LA (2021) Self-sensing active control of emulated tangential tool vibration hardware-in-the-loop. Control Eng Pract 109:104729
11. Suyama DI, Diniz AE (2020) Influence of tool vibrations on tool wear mechanisms in internal turning of hardened steel. J Braz Soc Mech Sci Eng 42(7):1–17
12. Lawrance G, Paul PS, Vasanth XA, Varadarajan AS, Daniel E (2019) Influence of magnetorheological elastomer on tool vibration and cutting performance during boring of hardened AISI4340 steel. J Mech Sci Technol 33(4):1555–1561
13. Wu J, Yu G, Gao Y, Wang LP (2018) Mechatronics modeling and vibration analysis of a 2-DOF parallel manipulator in a 5-DOF hybrid machine tool. Mech Mach Theory 121:430–445
14. Wu J, Wang JS, Wang LP, Li TM (2009) Dynamics and control of a planar 3-DOF parallel manipulator with actuation redundancy. Mech Mach Theory 44(4):835–849
15. Yu G, Wang LP, Wu J (2018) Prediction of chatter considering the effect of axial cutting depth on cutting force coefficients in end milling. Int J Adv Manuf Technol 96(9–12):3345–3354
16. Shirase K, Sano M, Hirao M, Yasui T (1998) Analysis and suppression of chatter vibration in end milling operation (lst Report). J Precis Eng Soc 64(3):465–469
17. Tang AM (2012) Research on a New type of high-speed end mill based on cutting stability. Doctoral dissertation of Hunan University. Hunan University
18. Sellmeier K, Denkena B (2011) Stable islands in the stability chart of milling proeesses due to unequal tooth pitch. Int J Mach Tools Manuf 51:152–164
19. Yusoff AR, Sims ND (2011) Optimisation of variable helix tool geometry for regenerative chatter mitigation. Int J Mach Tools Manuf 51:133–141
20. Otto A, Rauh S, Ihlenfeldt S, Radons G (2017) Stability of milling with non-uniform pitch and variable helix tools. Int J Adv Manuf Technol 89:2613–2625
21. Huang PL (2011) Research on variable pitch end mill for titanium alloy milling. Doctoral dissertation of Shandong University. Shandong University
22. Jin G (2013) Theoretical and experimental study on cutting stability of variable pitch variable spiral milling cutter. Doctoral dissertation of Tianjin University. Tianjin University
23. Alex I, Zoltan (2018) Optimum selection of variable pitch for chatter suppression in face milling operations. Materials 1(12):112
24. Song QH, Ai X, Zhao J (2011) Design for variable pitch end mills with high milling stability. International J Adv Manuf Technol 55:891–903
25. Rice JA (2011) Mathematical Statistics and Data Analysis. Mach Ind Press 102–105

Publisher's Note Springer Nature remains neutral with regard to jurisdictional claims in published maps and institutional affiliations.